Co$_2$YZ (Y= Cr, Nb, Ta, V and Z= Al, Ga) Heusler alloys under the effect of pressure and strain

Sadia Tabassam [a], Ali H. Reshak [b, c, d, *], G. Murtaza [e, f], S. Muhammad [a], A. Laref [g], Masood Yousaf [h], AM Mustafa Al Bakri [d], J. Bila [c]

[a] Materials Modeling Lab, Department of Physics, Hazara University, Mansehra, P. O. Box 21120, Pakistan
[b] Physics Department, College of Science, University of Basrah, Basrah, Iraq
[c] Department of Instrumentation and Control Engineering, Faculty of Mechanical Engineering, CTU in Prague, Technicka 4, Prague, 6 166 07, Czech Republic
[d] Center of Excellence Geopolymer and Green Technology, School of Material Engineering, University Malaysia Perlis, 01007, Kangar, Perlis, Malaysia
[e] Materials Modeling Lab, Department of Physics, Islamia College Peshawar, P.O. Box 25120, Pakistan
[f] Department of Mathematics & Natural Sciences, Prince Mohammad Bin Fahd University, P. O. Box 1664, Alkhobar, 31952, Saudi Arabia
[g] Department of Physics, College of Science, Imam Abdulrahman Bin Faisal University, P.O. Box 1982, 31441, City Dammam, Saudi Arabia
[h] Department of Physics, University of Education, Lahore, Pakistan

ARTICLE INFO

ABSTRACT

Full Heuslers alloys are a fascinating class of materials leading to many technological applications. These have been studied widely under ambient conditions. However, less attention been paid to study them under the effect of compression and strain. Here in this work Co$_2$YZ (Y= Cr, Nb, Ta, V and Z = Al, Ga) Heusler alloys have been studied comprehensively under pressure variations. Calculated lattice constants are in reasonable agreement with the available data. It is determined that lattice constant deceases with the increase in tensile stress and increases by increasing pressure in reverse direction. Band profiles reveals the half metallic nature of the studied compounds. The bond length decreases while band gap increases in compressive strain. The compounds are found to be reflective in visible region, as characteristics of the metals. The magnetic moments reveal the half-mettalic ferromagnetic nature of the compounds.

1. Introduction

For the development of novel materials in robotics and for applications in engineering, reversible structural deformations hold interest. Such deformations with strains are possessed by shape memory alloys [1]. The shape memory effect in most of materials is related to a martensitic phase transformation which is driven by temperature. The magnetic control of such transformations would be faster and more efficient [2]. For Heusler alloys this hold enough competency.

Heusler alloys are composed of metals, which in their pure state, are otherwise nonmagnetic. A German mining engineer and chemist named Fritz Heusler, in 1903, reported the possibility of making ferromagnetic alloys from non-ferromagnetic elements [3]

like copper, manganese, bronze and group B elements like aluminium, tin, arsenic, antimony and bismuth [4]. Heusler alloys are commonly classified as intermetallic compounds at the stoichiometric composition X$_2$YZ where X and Y are transition metals and Z is sp element [5] with X$_2$YZ having the L$_{21}$ structure (Full Heusler) and XYZ with the C$_{1b}$ structure (Half Heusler or semi-Heusler). Both Full Heusler and Half Heusler alloys generally exhibit cubic structure with F-43m (No = 216) space group. While Full Heusler compounds with composition X$_2$YZ can be converted to Half Heusler with composition XYZ, by decreasing the symmetry [6]. These compounds are half metallic showing metallic behavior in majority spin and semiconducting behavior in minority spin with 100% spin polarization at Fermi level. These compounds show high magnetic moments and Curie temperature which make them significant as magnetic materials [7].

Co$_2$VAl has been studied for its theoretical and experimental aspects. Experiments on Co$_2$VAl show that it has a magnetic moment of 1.4μ_B/cell [8]. Curie temperature of 342.7 K and lattice constant of 5.756 A° has been reported [9] conclusively making it

suitable for spintronics devices. The experimental lattice constant of Co_2VGa is found to be 5.792 Å which is in good agreement with the previous work [10]. For Co_2VGa, the magnetization at 5 K reveals its ferromagnetic behavior. The magnetic moment has a value of 2.04 μ_B/f.u [11]. The result is a consequence of half metallic electronic structure of this compound. The experimental lattice constants of Co_2CrAl is 5.727 Å while its magnetic moment is 1.55 μ_B [12] and Co_2CrGa has a lattice constant of 5.805 Å and a magnetic moment of 3.01 μ_B [13], respectively. These alloys are iso electronic; they have identical band structure having Curie temperatures of 330 K and 490 K [14]. A lattice parameter of 5.9579 Å and Curie temperature of 351 K is found for Co_2NbGa. The spontaneous magnetic moment per formula unit of Co_2NbGa at 5 K was found to be 1.81 μ_B [15]. Electronic properties of Co_2TaGa is predicted to be half metallic ferromagnetic with indirect band gap and 100% spin polarization. Lattice constants of Co_2TaAl and Co_2TaGa are 5.95 Å and 5.93 Å. The magnetic moment of Co_2TaGa is 2.0 μ_B [16]. Co based Heusler alloys hold an attractive potential for spintronics applications as in non-volatile random access memories, holding tendency for increased efficiency of optoelectronic devices and also having some potentials for self-assembled quantum computers [17]. Some other potential applications include tunneling magnetoresistance (TMR) and Giant magnetoresistance (GMR) elements and electro-mechanical uses [18]. The calculated spin-polarized electronic band structure for spin up, the majority spin and spin down the minority spin show that minority spin exhibits indirect band gap of about 0.3 eV for Co_2VAl and 0.2 eV for Co_2VGa. The values obtained by using GGA + U are much better than the previous calculated energy band gap 0.238 eV (0.189 eV) of Co_2VAl (Co_2VGa) using LDA + U [19]. Whereas the majority spin exhibit metallic structure with a density of states at EF, N(EF), of about 15.30 (state/eV/unit cell) for Co_2VAl and 13.22 (state/eV/unit cell) for Co_2VGa. The calculated density of states at EF enabled to calculate the bare electronic specific heat coefficient (γ) which is about 2.65 and 2.29 mJ/(mol cell K^2) for Co_2VAl and Co_2VGa [20]. The magnetic hyperfine effects were measured for Co_2CrAl, Co_2TaAl, Co_2VGa and Co_2NbGa Heusler alloys by TDPAC measurements [21]. Density functional based theoretical calculations were performed on Co_2YZ (Y=Sc, Cr and Z = Al, Ga) Heusler alloys by Li et al., [22]. It is found that the spin polarization of Co_2CrZ at Fermi level raises considerably, and Co_2ScZ keeps the non-magnetic feature when the external pressure increases. Thermodynamic calculations under the effect of temperature and pressure suggested the good thermodynamic properties of these compounds. Through the pseudopotential electronic method different physical properties of Co_2VAl were studied by Nepal et al., [23]. The role of electronic correlation effects was described in good detail. Co_2YAl (Y=Zr, Nb, Hf) were studied within GGA for electronic and magnetic properties by Rai et al., [24]. Compounds were revealed to be half-metallic ferromagnets (HMF). All of the compounds Co_2YAl (Y=Zr, Nb, Hf) shows the energy gaps at the Fermi level in spin down channel. We have also found that the increase in the total magnetic moments as the number of valence electrons increases. The calculated magnetic moments of Co_2YAl (Y=Zr, Nb, Hf) are an integer value.

Co_2YZ (Y= Cr, Nb, Ta, V and Z = Al, Ga) Heusler alloys have been studied due to their environmental friendliness, temperature stability and tendency of being half metallic. However, no considerable attention was paid to study of their behavior under strain and reduced pressures which are the useful tools in improving the performance of the devices due to changed band gap, electron mobility. Less theoretical investigations on these compounds motivated us to carryout current research work. Also the effect of stress and tension on the compounds could change their behavior. It is therefore very interesting to study these materials using the

state of the art first principles method. First principles methods now a days gain rapid reputation due to the less expensive and timely results production. Further there is no experimental (or theoretical) data required for the production of physical properties of any kind of materials.

2. Computational details

WIEN2k code [25] is used for the present calculations. FP-LAPW + lo (full potential linearized augmented plane wave plus local orbitals) method is used to depict the wave function and eigenvalues [26]. In this scheme unit cell is divided in two parts. One is the spherical region which represent the core states and include the atomic nuclei and electrons near to it. The electronic states in region is represented by the spherical harmonics multiplied by the atomic orbitals. The atomic radii of the spherical region is known as the mufftintin radii (Rmt). In the present calculations R_{MT} is choose in such a way that no charge leakage occurred. The Rmt for all the compounds and elements is provided in Table 1. The maximum orbital momentum l value for partial waves used inside atomic spheres is 10 as given in Table 1. The other region is the interstitial region which represent the valence states. The plane waves are used as a basis to produce the wave function expansion. The largest vector G in the Fourier expansion of the product of two orbitals and the generated potential in the interstitial region is 12. The Brilluion zone integrations is performed at the 1000 k-points. Rmt-Kmax determines matrix size (convergence), where Kmax is the plane wave cut-off, Rmt is the smallest of all atomic sphere radii. Here a value of 7 is used. The core and valence states generated are also given in Table 1. Along with GGA, Hubbard potential U parameter is also included to make the on-site coulombic correction with a value of 0.52 Ry., which is appropriate for most of materials.

3. Results and discussion

3.1. Electronic properties

3.1.1. Electronic band structure

The electronic band structure of a material decides electronic behavior of material (metallic or semiconductor). Electronic bands which are formed due to electron diffraction are classified as conduction bands and valence bands and the separation between these gaps is termed as energy band gap. The band gap may be direct or indirect depending whether the valence band maximum and the conduction band minimum lie at the same symmetry points of Brillion zone (in which case the band is direct) or lie at different points (in which case the band gap is indirect) and the material is then termed as indirect band gap material. These Heusler alloys have cubic structures with lattice constants of 5.682, 5.6982, 5.962, 5.960, 5.951, 5.949, 5.747 and 5.756 Å for Co_2CrAl, Co_2CrGa, Co_2NbAl, Co_2NbGa, Co_2TaAl, Co_2TaGa, Co_2VAl and Co_2VGa respectively. Fig. 1(a−d) shows the band structures of Co_2CrAl, Co_2CrGa, Co_2NbAl and Co_2NbGa calculated by GGA approximation for Non-spin case. Metallic structure is obvious from the merging of valence and conduction bands at the Fermi Level. Fig. 1(e−h) represents the band structures of these compounds for spin-polarized case. Spin up channel shows metallic behavior while spin down channel is semiconducting. Fig. 1(i−m) shows energy gaps between the valence and conduction bands with a band gap of 0.72 eV respectively for Co_2CrAl, 0.73 eV for Co_2CrGa, 0.80 eV for Co_2NbAl, 0.45 eV for Co_2NbGa. Fig. 2(a−d) shows band structures of Co_2TaAl, Co_2TaGa, Co_2VAl and Co_2VGa having lattice constants of 5.95, 5.94, 5.74 and 5.75 Å respectively. Metallic character can be seen in Fig. 2(e−h) for Non-Spin channel while semiconducting behavior is obvious in Fig. 4(i−m) with band gaps of 0.76 eV for Co_2TaAl,

Table 1
Computational parameters used for this study.

	RK_{max}	L_{max}	G_{max}	R_{MT}	k-points	Core States	Valence States
Co_2CrAl	7	10	12	Co = 2.37, Cr = 2.25, Al = 2.14	1000	1s, 2p, 3s	3p, 3d, 4s
Co_2CrGa	7	10	12	Co = 2.38, Cr = 2.26, Ga = 2.26	1000	1s, 2s, 2p	3s, 3p, 3d, 4s
Co_2NbAl	7	10	12	Co = 2.48, Nb = 2.36, Al = 2.24	1000	1s, 2s	2p, 3s,
Co_2NbGa	7	10	12	Co = 2.48, Nb = 2.36, Ga = 2.36	1000	1s, 2s, 2p, 2s, 3p	3d, 4s
Co_2TaAl	7	10	12	Co = 2.42, Ta = 2.42, Al = 2.24	1000	1s, 2s, 2p, 3s, 3p, 3d, 4s, 4p	5s, 5p, 4f, 5d, 6s
Co_2TaGa	7	10	12	Co = 2.42, Ta = 2.42, Ga = 2.36	1000	1s, 2s, 2p,3s, 3p	3d, 4s
Co_2VAl	7	10	12	Co = 2.39, V = 2.28, Al = 2.16	1000	1s, 2s, 2p	3s, 3p, 3d, 4s
Co_2VGa	7	10	12	Co = 2.4, V = 2.28, Ga = 2.28	1000	1s, 2s, 2p, 3s, 3p	3d, 4s,
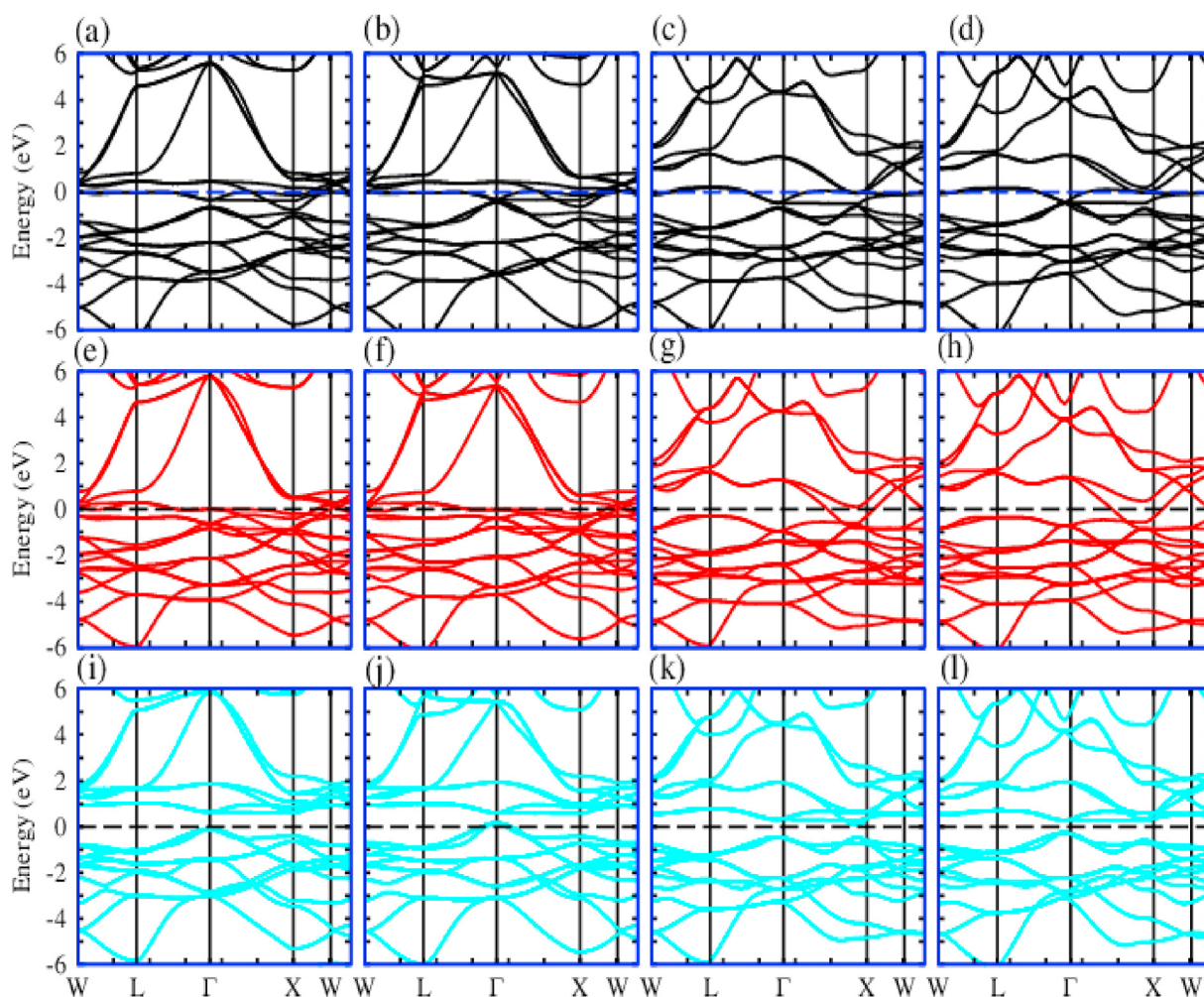
Fig. 1. Electronic band structure of Co_2CrAl, Co_2CrGa, Co_2NbAl, and Co_2NbGa for non-spin, spin up and spin down states using GGA.

0.51 eV for Co_2TaGa, 0.76 eV for Co_2VAl and 0.52 eV for Co_2VGa respectively. All these materials are found to be direct band gap materials having both valence band maximum and conduction band minimum at Γ point.

Calculation for electronic properties by the use GGA + U shows that these compounds show metallicity for non-spin (Fig. 3(a−d)) as well as spin-up channel (Fig. 3(e−h)) and are semiconducting for spin-down channel and show band gaps of 0.75 eV for Co_2CrAl, 0.753 eV for Co_2CrGa, 0.78 eV for Co_2NbAl, 0.84 eV for Co_2NbGa as shown in Fig. 3(i−l), which show their half metallic nature. Similarly, the compounds Co_2TaAl, Co_2TaGa, Co_2VAl and Co_2VGa show half metallic characters with merging of valence and conduction bands Fig. 4(a−h) and having band gaps of 0.77 eV, 0.51 eV, 0.76 eV

and 0.52 eV in Spin-Down Channel as shown in Fig. 4(i−l).

3.1.2. Electronic band structure under tensile stress and strain

Electronic band structures of the compounds were probed under the compressive stress of 2 GPa, 4 GPa, 6 GPa, 8 GPa, 10 GPa and under tensile strain of -2GPa, -4 GPa, -6 GPa, -8 GPa and −10GPa. For non-spin channel, all the compounds show the metallic nature under the stress and strain conditions when no spin polarization is considered. Further, all the compounds reveal metallic nature under effect of stress and strain in the spin up state. The compounds show semiconducting nature in the spin down state. So all the compounds retain the half-metallic nature in the pressure range -10 − 10 GPa. The calculated lattice constants and energy bandgaps
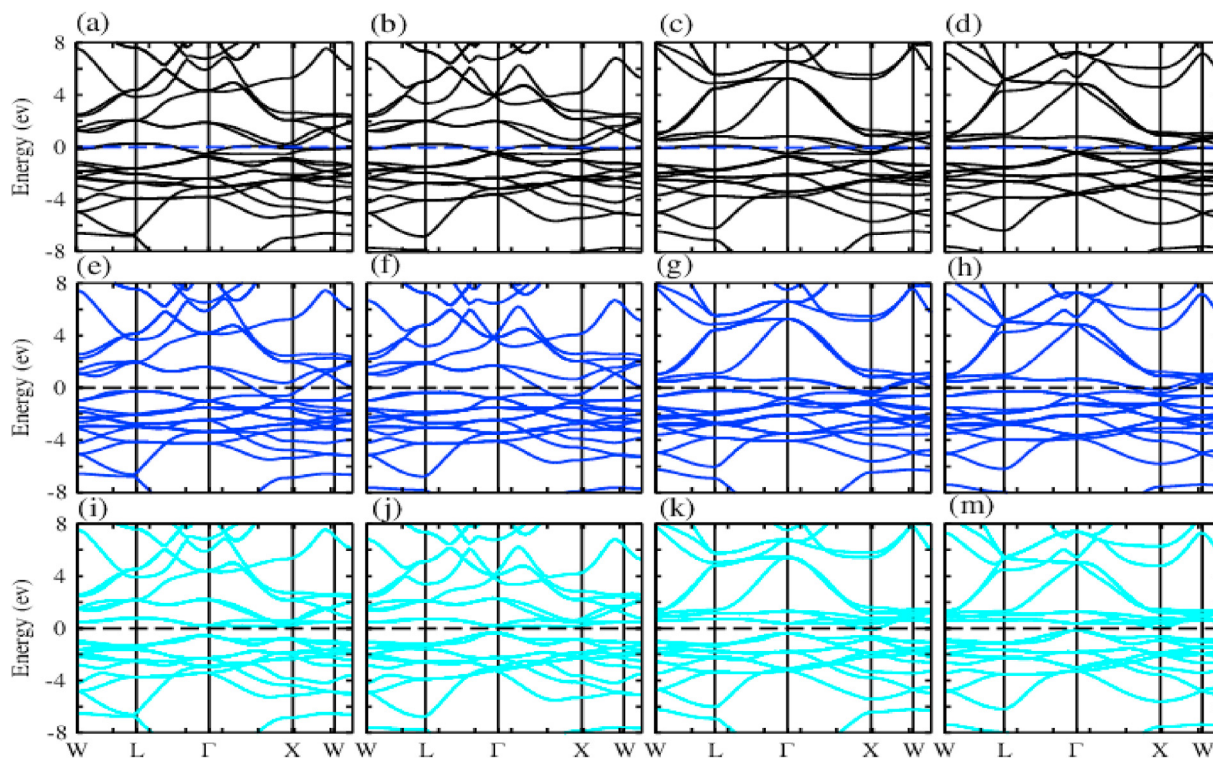
Fig. 2. Electronic Band Structure of Co_2TaAl, Co_2TaGa, Co_2VAl, Co_2VGa for non-spin, spin up and spin down states using GGA.
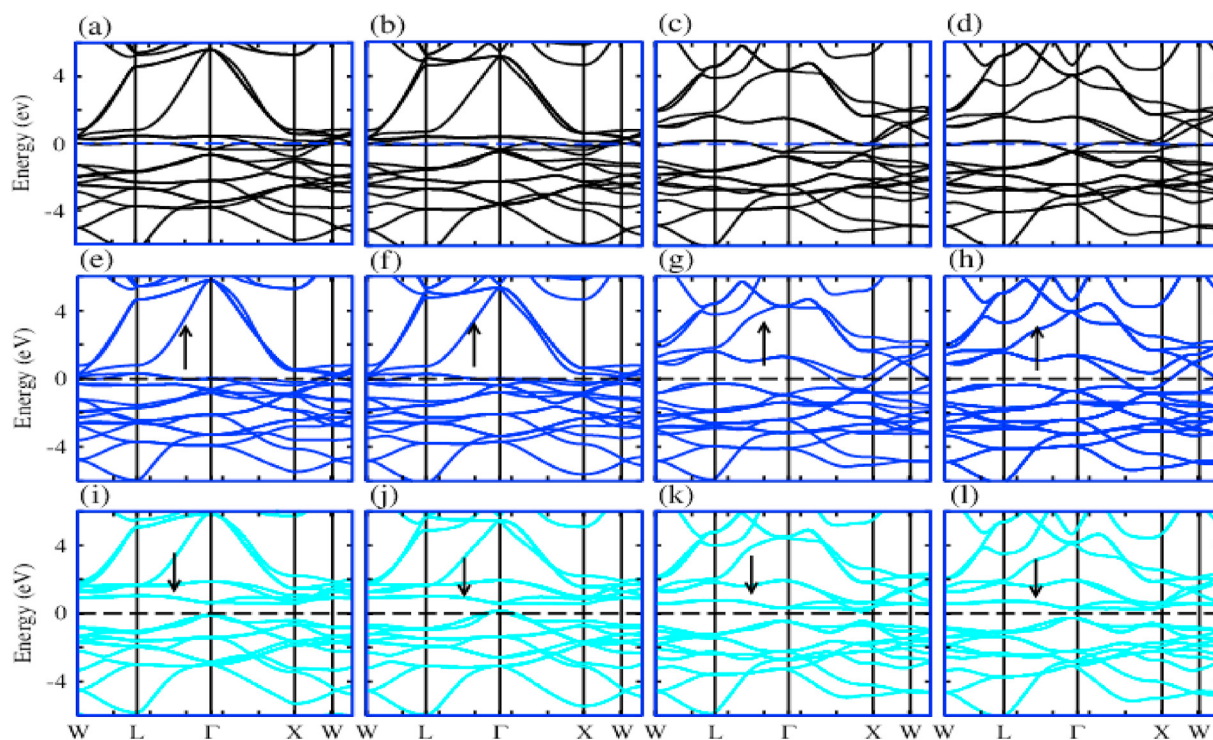
Fig. 3. Electronic Band Structure of Co_2CrAl, Co_2CrGa, Co_2NbAl, Co_2NbGa for non-spin, spin up and spin down states using GGA + U.

are depicted in Table 2.

For the case of Co_2CrAl, it shows semiconducting properties with band gaps of 0.71 eV, 0.82 eV, 0.77 eV, 0.78 eV and 0.79 eV for 2 GPa, 4 GPa 6 GPa, 8 GPa and 10 GPa respectively. The maximum band gap is recorded for the case of 4 GPa. It shows direct bands gaps of 0.77 eV for -2GPa, 0.75 eV for -4GPa, 0.71 eV for -6GPa, 0.72 eV for -8GPa and 0.72 eV for −10GPa respectively, in spin down channel. The smallest value of band gap occurs at -4GPa. For the
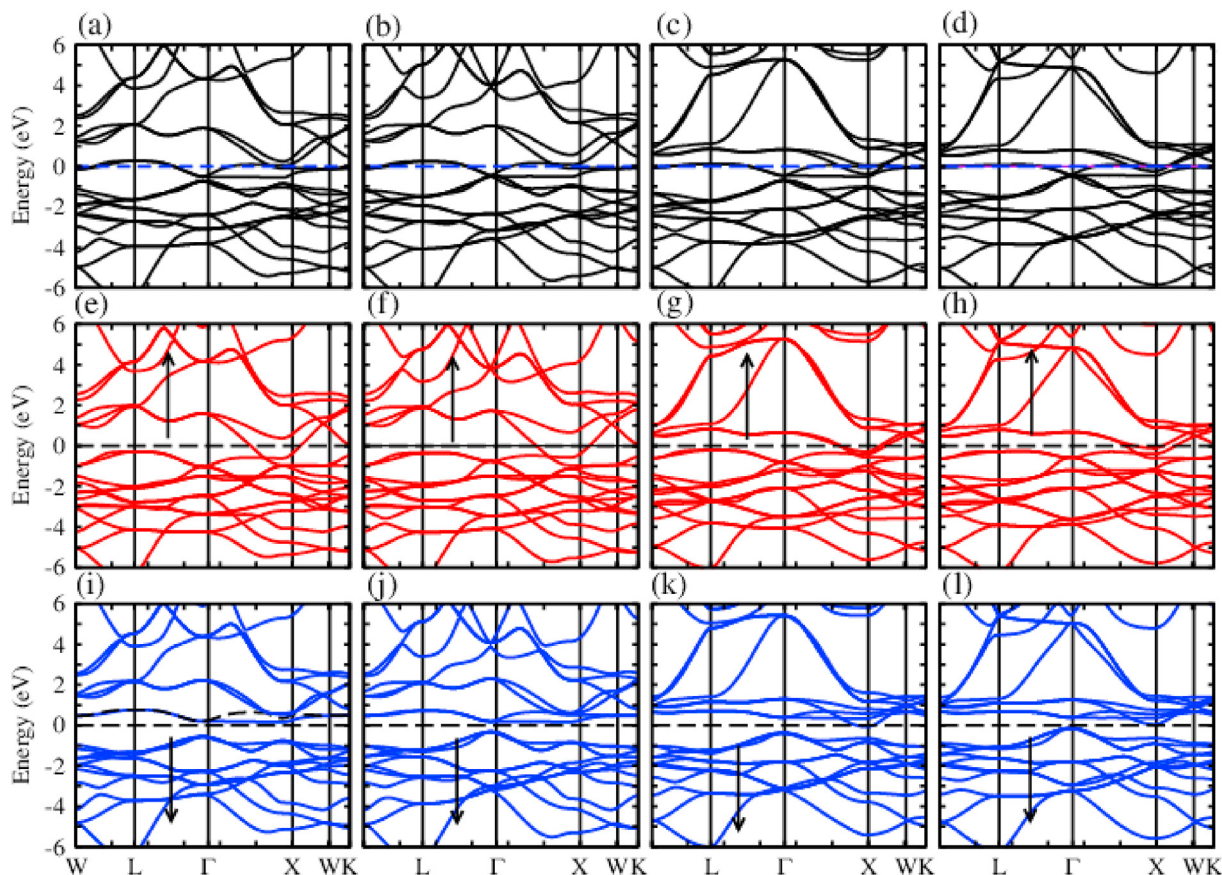
Fig. 4. Electronic Band Structure of Co$_2$TaAl, Co$_2$TaGa, Co$_2$VAl, Co$_2$VGa for non-spin, spin up and spin down states using GGA + U.

case of Co$_2$CrGa, the compound appears to be semiconducting for spin down channel with band gaps of 0.72eV, 0.81eV, 0.68eV, 0.65eV and 0.63eV for 2 GPa, 4 GPa, 6 GPa, 8 GPa and 10 GPa while the tensile strain of -2GPa, -4 GPa, -6 GPa, -8 GPa and −10 GPa have band gaps of 0.75eV, 0.77eV, 0.79eV, 0.81eV and 0.84eV respectively. The maximum band gap of 0.81eV is recorded for 4 GPa pressure.

Electronic band structure of Co$_2$NbAl reveals semiconducting behavior in spin down state. The band gaps of Co$_2$NbAl under spin down channel are 0.78eV for 2 GPa, 0.79eV for 4 GPa, 0. 79eV for 6 GPa, 0.79eV for 8 GPa and 0.80eV for 10 GPa respectively. The band gap is increasing with pressure while lattice constants are decreasing. The results agree with the zero pressure energy bandgap of 0.65 eV in spin down state [24]. It shows band gaps of 0.78 eV, 0.77eV, 0.76eV, 0.76eV, 0.75eV for -2GPa, -4 GPa, -6 GPa, -8 GPa and −10GPa. The bands gap decreasing with decreasing pressure while lattice constants are found to be increasing with a decrease of pressure. In the case of Co$_2$NbGa, it shows band gaps of 0.55eV, 0.55eV, 0.54eV, 0.55eV and 0.55eV for 2 GPa, 4 GPa, 6 GPa, 8 GPa and 10 GPa respectively. Under tensile strain of -2GPa to −10GPa, the compound shows metallic behavior in spin up channel and semiconducting behavior in spin down channel hence proved to be half metal, with band gaps of 0.549eV, 0.548eV, 0.547eV, 0.546eV, 0.547eV for -2GPa, -4 GPa, -6 GPa, -8 GPa and −10GPa, respectively.

For compound Co$_2$TaAl when pressure increased energy band gap also increased in the spin down state. Increasing the pressure show the decrease of lattice constants. When the pressure applied in the reverse direction, energy band gap decreased. For Co$_2$TaGa, when pressure is increased from 2 GPa to 10 GPa, the compound showed to be metallic under spin-up channel while

semiconducting under spin-down channel. In spin-down channel, gap was found to be 0.52eV and remain same when the pressure was increased to 10 GPa. By releasing the pressure from -2GPa to −10GPa, the compound showed its metallic nature in spin up channel while it showed semiconducting nature for pressures of -2GPa, -4 GPa, -8 GPa and −10GPa having band gaps of 0.52eV i.e the band gap remained the same with decrease in pressure except for -6GPa where the compound appeared to be metallic with its valence band crossing the Fermi level.

Co$_2$VAl show energy band gaps of 0.78eV for 2 GPa, 0.77eV for 4 GPa, 0.77eV for 6 GPa, 0.78eV for 8 GPa and 0.79eV for 10 GPa respectively. The band gap is found to be decreasing with increase of pressure. In the negative pressure range, it showed energy gaps of 0.76eV, 0.74eV, 0.73eV 0.75eV and 0.74eV for -2GPa, -4 GPa, -6 GPa, -8 GPa and −10GPa respectively. So, the band gap is found to be increasing with the reduction of pressure. For spin polarized calculations of Co$_2$VGa, the metallic behavior is observed in spin up channel when pressure is increased from 2 GPa to 10 GPa and a semiconducting behavior is observed for spin-down channel with band gaps of 0.519eV, 0.516eV, 0.52eV, 0.521eV and 0.52 eV for 2 GPa, 4 GPa, 6 GPa, 8 GPa and 10 GPa respectively. The decrease in pressure from -2GPa to −10GPa revealed the metallic character of Co$_2$VGa for spin-up channel and its semiconducting nature for spin-down channel with band gaps of 052eV, 0.53eV, 0.52eV, 0.54eV and 1.42eV for -2GPa, -4 GPa, -6 GPa, -8 GPa and −10GPa.

3.2. Density of states

To further analyze the electronic band structure, we have calculated partial density of states. The partial density of states provides a detailed information about contribution of each orbital

Table 2

Calculated structural parameters and energy band gap of Heuslers under compressive and tensile strain.

Compressive Stress (GPa)	Lattice Constant (Å)	Band-Gap (eV)	Tensile Strain (GPa)	Lattice Constant (Å)	Band-Gap (eV)
Co$_2$CrAl					
2	5.67	0.71	−2	5.70	0.77
4	5.65	0.82	−4	5.72	0.75
6	5.64	0.77	−6	5.74	0.71
8	5.62	0.78	−8	5.76	0.72
10	5.61	0.79	−10	5.79	0.72
Co$_2$CrGa					
2	5.69	0.72	−2	5.72	0.75
4	5.74	0.81	−4	5.74	0.74
6	5.65	0.68	−6	5.76	0.76
8	5.64	0.65	−8	5.78	0.78
10	5.62	0.63	−10	5.80	0.80
Co$_2$NbAl					
2	5.94	0.78	−2	5.98	0.78
4	5.92	0.78	−4	6.00	0.77
6	5.90	0.79	−6	6.02	0.76
8	5.89	0.79	−8	6.04	0.76
10	5.87	0.80	−10	6.07	0.75
Co$_2$NbGa					
2	5.94	0.551	−2	5.98	0.549
4	5.92	0.556	−4	6.00	0.548
6	5.90	0.548	−6	6.02	0.547
8	5.89	0.552	−8	6.04	0.546
10	5.87	0.551	−10	6.06	0.547
Co$_2$TaAl					
2	5.93	0.77	−2	5.96	0.76
4	5.91	0.78	−4	5.98	0.76
6	5.89	0.78	−6	6.01	0.76
8	5.88	0.78	−8	6.03	0.75
10	5.86	0.79	−10	6.05	0.74
Co$_2$TaGa					
2	5.93	0.52	−2	5.96	0.52
4	5.91	0.52	−4	5.98	0.52
6	5.90	0.52	−6	5.90	Metallic
8	5.88	0.52	−8	6.028	0.52
10	5.87	0.52	−10	6.051	0.52
Co$_2$VAl					
2	5.72	0.78	−2	5.76	0.76
4	5.71	0.77	−4	5.78	0.74
6	5.69	0.77	−6	5.80	0.73
8	5.68	0.78	−8	5.82	0.75
10	5.66	0.79	−10	5.85	0.74
Co$_2$VGa					
2	5.73	0.519	−2	5.67	0.52
4	5.72	0.516	−4	5.79	0.53
6	5.70	0.52	−6	5.81	0.52
8	5.69	0.52	−8	5.83	0.54
10	5.67	0.52	−10	5.85	1.42

of different atoms in a material. The nature of the material (metallic or semiconductor) can be calculated by density of states. The valence band is at left side of the Fermi level having on negative x-axis while the right side of the Fermi level represents conduction band on positive x-axis.

Fig. 5(a−d) shows partial density of states of compounds Co$_2$CrAl, Co$_2$CrGa, Co$_2$NbAl and Co$_2$NbGa for non-spin channel while Fig. 5(e−h) shows partial density of states of these compound for spin-polarized state. All these compounds show metallic nature in non-spin channel as their orbitals are crossing Fermi level and shows the merging of these states in conduction and valence bands as shown in the figure. In Co$_2$CrAl (Fig. 5(a)) the metallic nature is due to d orbital of Cr and Co. the d-orbital is further split into three orbitals dx^2, dxy and dyz. For spin-polarized channel (Fig. 5(e)), the compound shows semiconducting nature as observed by the band gap at the Fermi level between the states. Co$_2$CrGa (Fig. 5(b)) shows its metallic nature in Non-Spin channel which is due to Co atom as its d-orbital is crossing Fermi level and the compound shows its semiconducting nature in spin-polarized channel have a band gap between its valence and conduction band. Similarly, Co₂NbAl

(Fig. 3(c)) and Co$_2$NbGa (Fig. 3(d)) also show metallic nature in their non-spin states and their metallic nature is mainly due to contribution of d-orbital of Co atom while in spin polarized state (Fig. 5(g)) and (Fig. 5(h)), both of these compounds behave as a semiconductor.

Fig. 6(a−d) shows partial density of states of Co₂TaAl, Co₂TaGa, Co₂VAl and Co₂VGa for non-spin state and their partial density of states in Fig. 6(e−h) for their spin-polarized states. All these compounds behave metallic in their non-spin state and semiconducting in their spin-polarized state as indicated by a band gap between the conduction and valence band. In Co₂TaAl, Co₂TaGa and Co₂VGa, the metallic nature is due to dx^2, dxy and dyz orbital of Co atom while in Co₂VAl the metallic state is due to contribution of d orbital of Co and V atom.

Fig. 7(a−d) shows the partial density of states as calculated by GGA + U potential for their spin polarized channels. Co₂CrAl (Fig. 9(a)) shows its metallic nature in spin up channel which is due to contribution of d orbitals of Co and Cr atoms while it shows semiconducting nature in spin down channel. Co₂CrGa (Fig. 9(b)) Co₂NbAl (Fig. 9(c)) Co₂NbGa (Fig. 9(d)) Co₂TaAl (Fig. 9(e)) Co₂TaGa
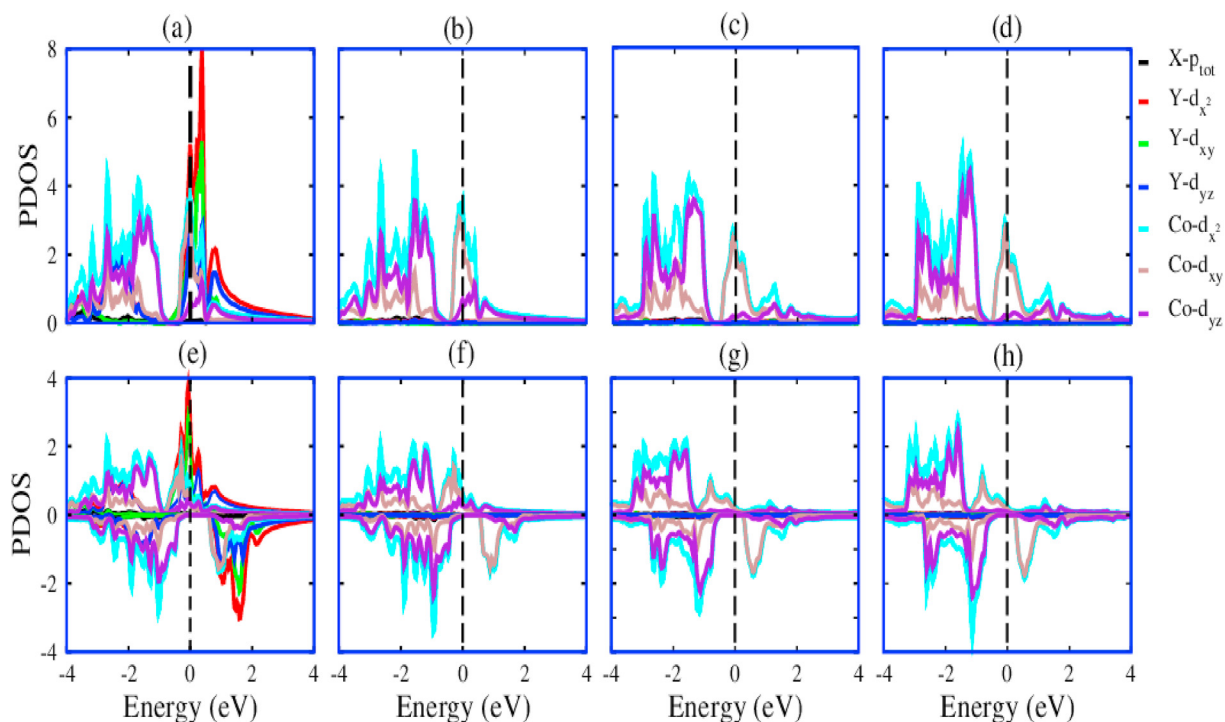
Fig. 5. Partial density of states of Co$_2$CrAl (a, e), Co$_2$CrGa (b, f), Co$_2$NbAl (c, g) and Co$_2$NbGa (d, h) for non-spin and spin polarized states.
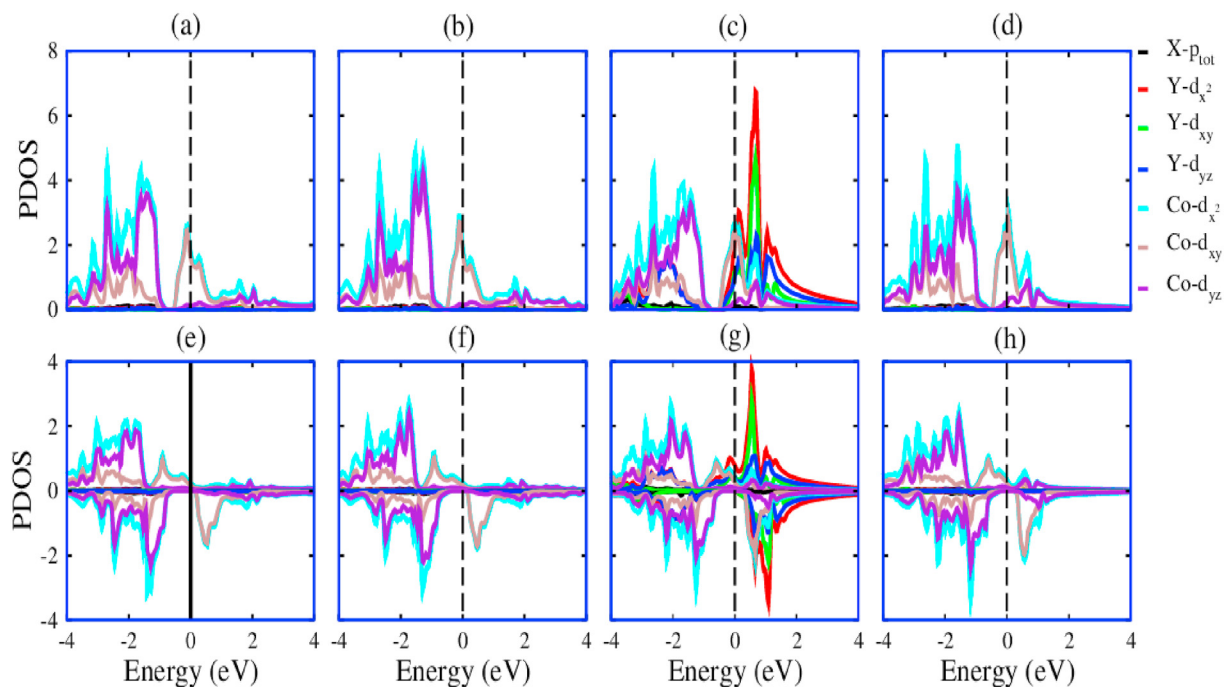
Fig. 6. Partial Density of States of Co$_2$TaAl (a, e), Co$_2$TaGa (b, f), Co$_2$VAl (c, g) and Co$_2$VGa (d, g) for non-spin and spin polarized states.

(Fig. 9(f)) and Co$_2$VGa (Fig. 9(h)) also show metallic nature in spin up state while semiconducting nature in spin down. The metallic nature of all these compounds is due to contribution of d-orbital of Co atom. Co$_2$VAl (Fig. 9(g)) also shows metallic nature in spin up channel which is due to d-orbital of V and Co atom and shows semiconducting behavior as observed by the band gap between the conduction band and the valence band in its spin down channel. All

these compounds are Heusler alloys as they are metallic in spin up state and become semiconducting in spin down state.

3.3. Density of states under compressive and tensile strain

Fig. 8 shows partial density of states of Co$_2$CrAl for non-spin polarization under increasing pressure from 2 GPa to 10 GPa and
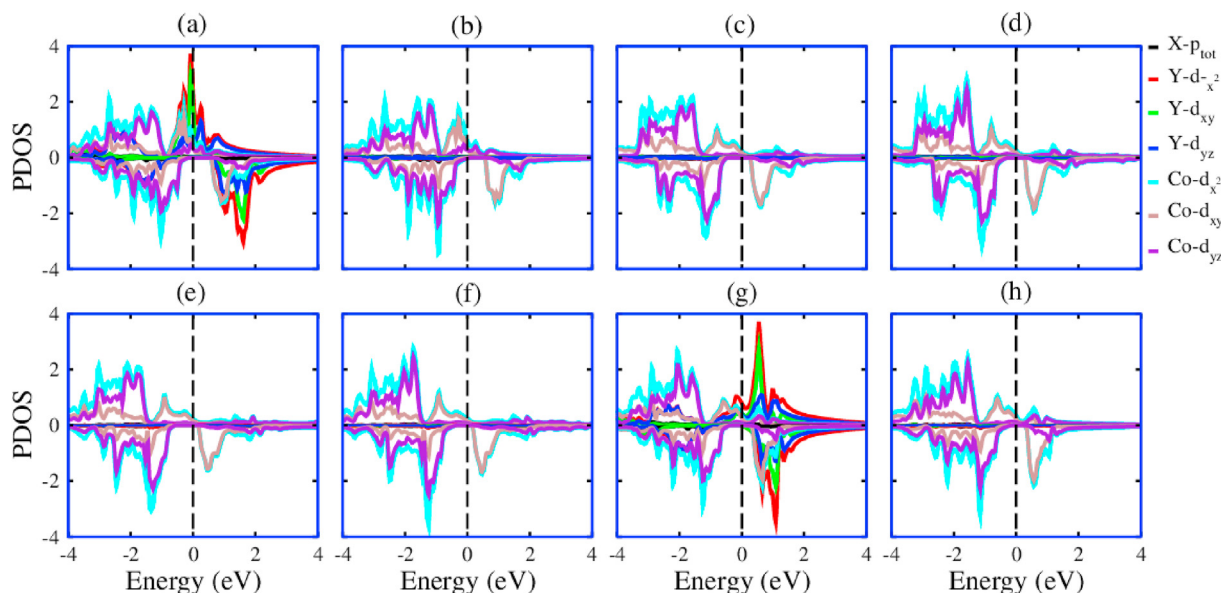
Fig. 7. Partial Density of States of Co_2CrAl, Co_2CrGa, Co_2NbAl, Co_2NbGa, Co_2TaAl, Co_2TaGa, Co_2VAl, Co_2VGa for Spin polarized States calculated with GGA + U.

then for decreasing pressures of -2GPa to −10GPa. Under all these conditions, the compounds show metallic behavior. The d-orbital of Co and Cr atoms are major contributors in metallicity. As all the compounds show metallic nature similar to Fig. 8, therefore other figures are not shown. The Partial density of states of Co_2CrAl under spin polarized channel also gives metallic behavior in spin up state with Co and Cr atom's d orbitals contributing in metallicity and semiconducting nature in spin down state showing a band gap. The partial density of states of Co_2CrGa under non-spin channel are also studied. When we increase the pressure from 2 GPa to 10 GPa, all these compounds showed metallicity under increasing pressure. The metallicity is due to the contributions of dx^2, dxy and dyz orbital of Co atom. For spin polarization, Co_2CrGa shows metallic nature under spin up channel and semiconducting nature under spin down channel as observed from the band gap between valence and conduction band.

Partial density of states of Co_2NbAl under non-spin channel shows metallic nature contributed by Co atom with its d orbital crossing the Fermi Level from valence band to conduction band. The pattern prevails for both increase and decrease of pressure respectively. Under spin polarized nature, we see metallicity under spin up state and semiconducting behavior under spin down state under both increasing and decreasing pressures. Under Non-Spin channel, Co_2NbAl behaves as metallic under both increasing and decreasing pressures, respectively. The d orbital (dx^2, dxy and dyz) are contributing in the metallicity of Co_2NbGa. Partial density of states of Co_2NbGa shows metallic nature under spin-up channel while a semiconducting nature is observed in spin-down state.

Partial density of states of Co_2TaAl, under non-spin channel, shows metallicity characterized by contribution of d orbital of Co atom under both increasing and decreasing pressures. Under spin-polarized state, the partial density of states proves the half metallicity of the compound as it is metallic under spin up channel and semiconducting in spin down channel under both increasing and decreasing pressures. Partial density of states of Co_2TaGa shows metallic character for non-spin channel. The metallicity is characterized by the contribution of Co-d orbital. The dx^2, dxy and dyz orbital cross the Fermi level thus showing a metallic behavior. In spin polarized channel, Co_2TaGa behaves as a half metal by showing metallicity in spin up state and showing semiconducting nature in

spin down state.

The metallic behavior of Co_2VAl is due to the contribution of split d orbital of Co and V atom. The orbital crosses the Fermi level thus making the compound metallic. In spin polarized channel, the compound appears to be metallic in spin up channel while semiconducting in spin down channel. The metallic behavior of Co_2VGa in non-spin state is contributed by the d orbital of Co atom. In spin polarized state, the half metallicity is caused by d orbital of Co atom which makes the material metallic in spin up channel while semiconductor in spin down channel having a band gap between valence and conduction band.

3.4. Optical properties

Optical Properties i.e reflectivity and conductivity of Co_2YZ (Y= Cr, Nb, Ta, V) (Z = Al, Ga) are discussed as follows:

3.4.1. Reflectivity

The plot for reflectivity as a function of frequency in Fig. S1 (supplementary materials) shows that Co_2CrAl, Co_2CrGa and Co_2NbAl show high reflectivity in low energy range (infrared) and show a sharp decrease in reflectivity towards high frequency. The large values of N (free electron densities) lead to plasma frequencies in ultraviolet region. The highest frequency with which light can be scattered (that is to say, reflect) is referred to as plasma frequency ω_p. With ω_p in ultraviolet region, the visible photons have frequencies below plasma frequency and thus ε_r is negative. This means up to plasma frequency the reflectivity is expected to be 100%. These compounds show increasing reflectivity in visible region after which the peaks start shifting down at higher energies due to the interband transitions. Co_2VGa shows relatively low reflectivity in ultraviolet region than aforementioned compounds. Co_2NbGa, Co_2TaAl, Co_2VAl show low reflectivity compared to other compounds with Co_2TaAl having least reflectivity in ultraviolet region. All these compounds, showing metallic nature (although electronically these materials are half-metals but for optical photons interaction of light matter is independent of spin), tend to be good reflectors at visible frequencies. Co_2VGa shows highest reflectivity in visible region which gradually decreases with higher energies which means that there is interband transitions in visible
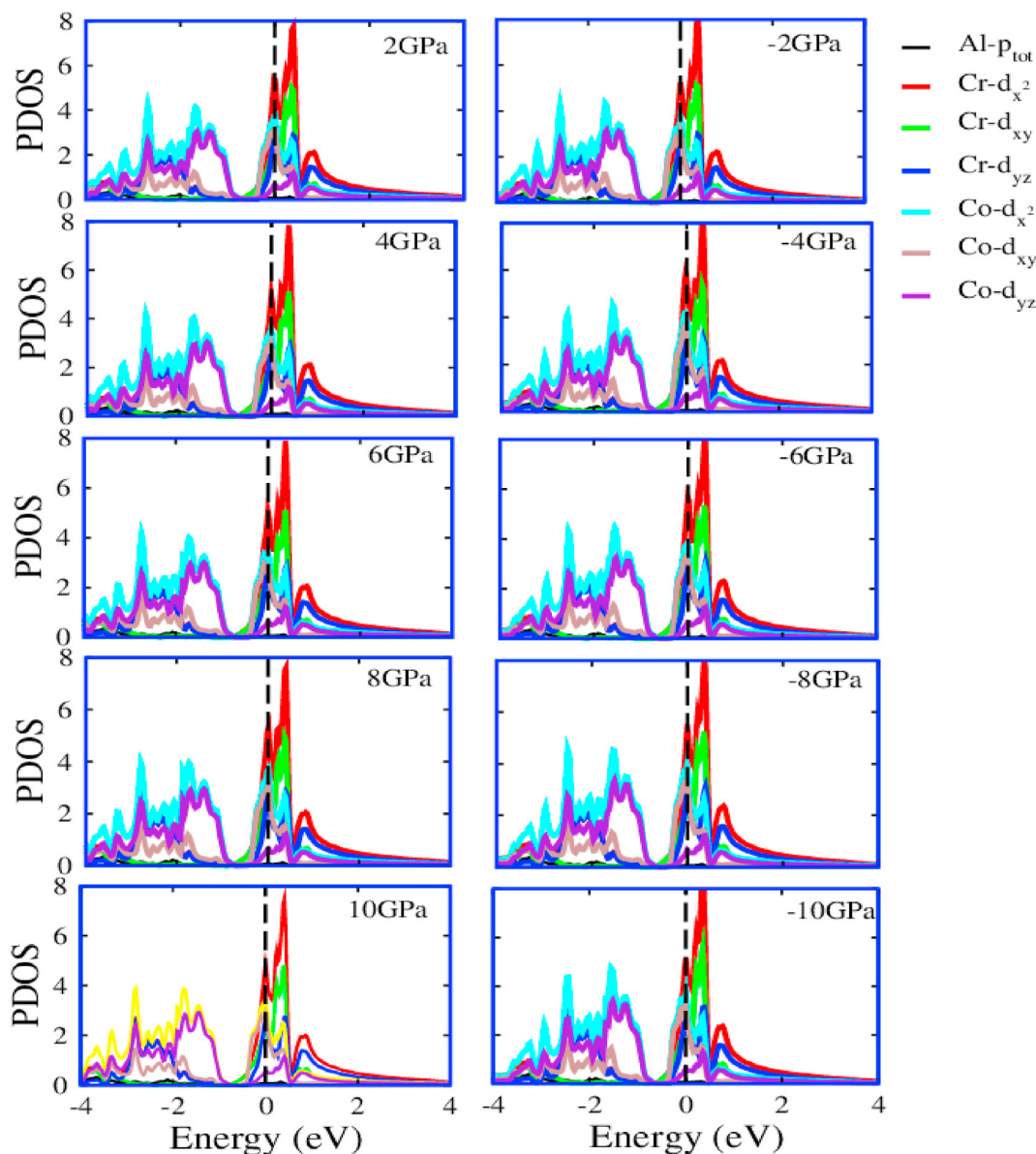
Fig. 8. Partial Density of States of Co$_2$CrAl under Compressive and Tensile Strain for non-spin state.

region. So these compounds may show characteristic colors. The reflectivity is slightly low in infrared region than ultraviolet and visible regions.

3.4.2. Reflectivity under pressure

The optical reflectivity of Co$_2$CrAl is also calculated under the effect of pressure and shown in Fig. S2. By increasing the pressure, the reflectivity of Co$_2$CrAl first increases slightly than the case with no pressure applied, in the visible region and then decrease sharply with increasing energy. The decrease in pressure also show larger reflectivity in ultraviolet region due to high electron density which decreases sharply and start increasing toward the visible region. The peaks show decrease in reflectivity towards higher energies. In higher energy ranges the peaks shift slightly toward higher reflectivity than the case when no pressure is applied. The optical reflectivity of Co$_2$CrGa is also calculated under the effect of pressure and shown in Fig. S3. The compound shows the reflectivity trend characteristic of metals which are good reflectors in visible and

ultraviolet regions. With the increase in pressure, the peak shifts to maximum at 4 GPa in ultraviolet region. With decrease in pressure, the same trend is maintained with high reflectivity in visible region which decreases with high energy and again showing reflectivity in ultraviolet region with peaks shifting toward higher values with decreasing pressure. The maximum reflectivity in ultraviolet region is for −10GPa pressure. The optical reflectivity of Co$_2$NbAl is also calculated under the effect of pressure and shown in Fig. S4. For both cases of pressure increase and decrease, the compound follows the same trend of reflectivity as characteristics of metals, having high reflectivity in visible and ultraviolet regions. The optical reflectivity of Co$_2$NbGa is also calculated under the effect of pressure and shown in Fig. S5. The reflectivity starts increasing towards the higher energies, having maximum value in visible region after which it starts decreasing towards higher energies again showing reflective behavior in ultraviolet region. The optical reflectivity of Co$_2$TaAl is also calculated under the effect of pressure and shown in Fig. S6. The compound is less reflective in visible and
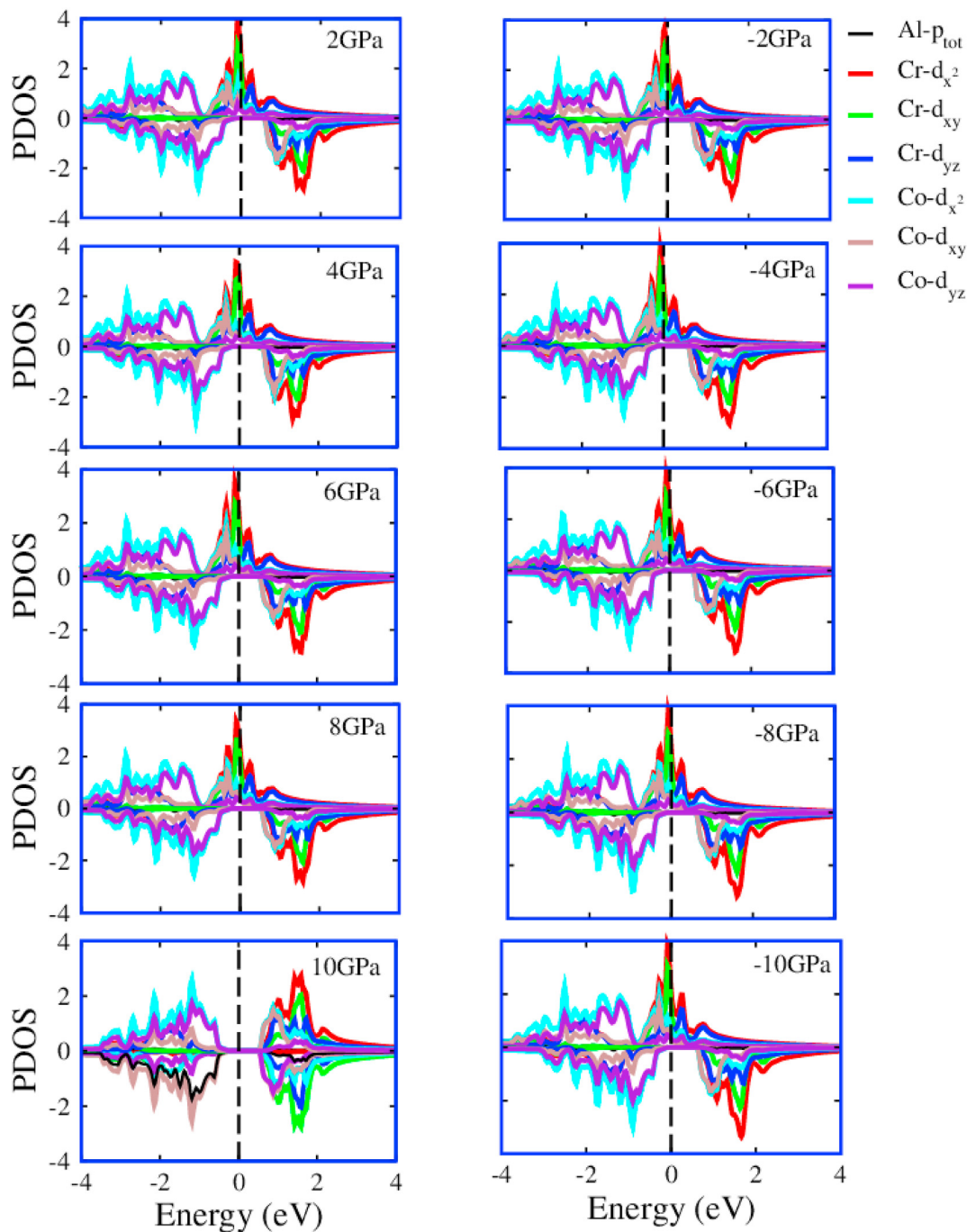
Fig. 9. Partial Density of States of Co$_2$CrAl under Compressive and Tensile Strain for Spin polarized state.

ultraviolet regions as compared to Co$_2$CrAl, Co$_2$CrGa which are highly reflective in Infrared regions as well. This compound show reflectivity increasing towards visible region with sharp reduction towards higher energies and again being reflective in ultraviolet region. The optical reflectivity of Co$_2$TaGa is also calculated under the effect of pressure and shown in Fig. S7. Co$_2$TaGa shows the reflectivity being maximum in visible range and slightly decreasing with high energies and then again increasing in ultraviolet regions with increasing pressures. With decreasing pressures, the same trend is maintained by the compound except for -6GPa for which the peak shifts toward higher values which may be due to high plasma frequency at this pressure. The optical reflectivity of Co$_2$VAl

is also calculated under the effect of pressure and shown in Fig. S8. The frequency dependent reflectivity increases from infrared toward ultraviolet region, the compound being highly reflective in visible region with decrease in energy towards higher energies and again being reflective in ultraviolet region for both increasing and decreasing pressure cases. The optical reflectivity of Co$_2$VGa is shown in Fig. S9. At 0 GPa, the reflectivity starts increasing towards visible range making the compound to be highly reflective in visible range. By increasing the Pressure up to 10 GPa shows the shift in the peaks of the compound toward lower reflectivity. The reflectivity is maximum in the visible range and decreases with the increase in energy. Decreasing the pressure again shows the decrease in

Table 3
Calculated total (M_{total}) and individual magnetic moments.

	M_{total} (GGA + U)	M_{total} other literature	m_A	m_B	m_C
Co_2CrAl	2.99	1.55[a], 3.00[b]	0.7	1.51	−0.05
Co_2CrGa	3.01	2.36[a], 3.05[b]	0.75	1.58	−0.05
Co_2NbAl	2.01	1.35[a], 2.00[b]	1.05	0.001	−0.07
Co_2NbGa	2.00	1.39[a], 2.00[b]	1.04	−0.017	0.002
Co_2TaAl	1.97	–	1.03	−0.020	0.001
Co_2TaGa	1.97	–	1.03	−0.037	0.01
Co_2VAl	1.97	1.95[a], 2.00[b]	0.93	0.21	−0.02
Co_2VGa	1.99	1.92[a], 2.01[b]	0.95	0.16	−0.016

[a] Represents the experimental results [30].
[b] Represents the theoretical results of other works [27].

reflectivity with increasing energy. The material is most reflective in visible range while also showing some reflectivity in infrared red.

3.5. Optical conductivity

The calculated optical conductivity at zero pressure is shown in Fig. S10. The conductivity starts increasing from infrared towards visible region and has maximum peak in visible region after which it starts decreasing towards higher energies. Co_2VGa is found to be the most conductive among all these compounds. The rest of the compounds have similar conductivity trends with slight shift in the peaks.
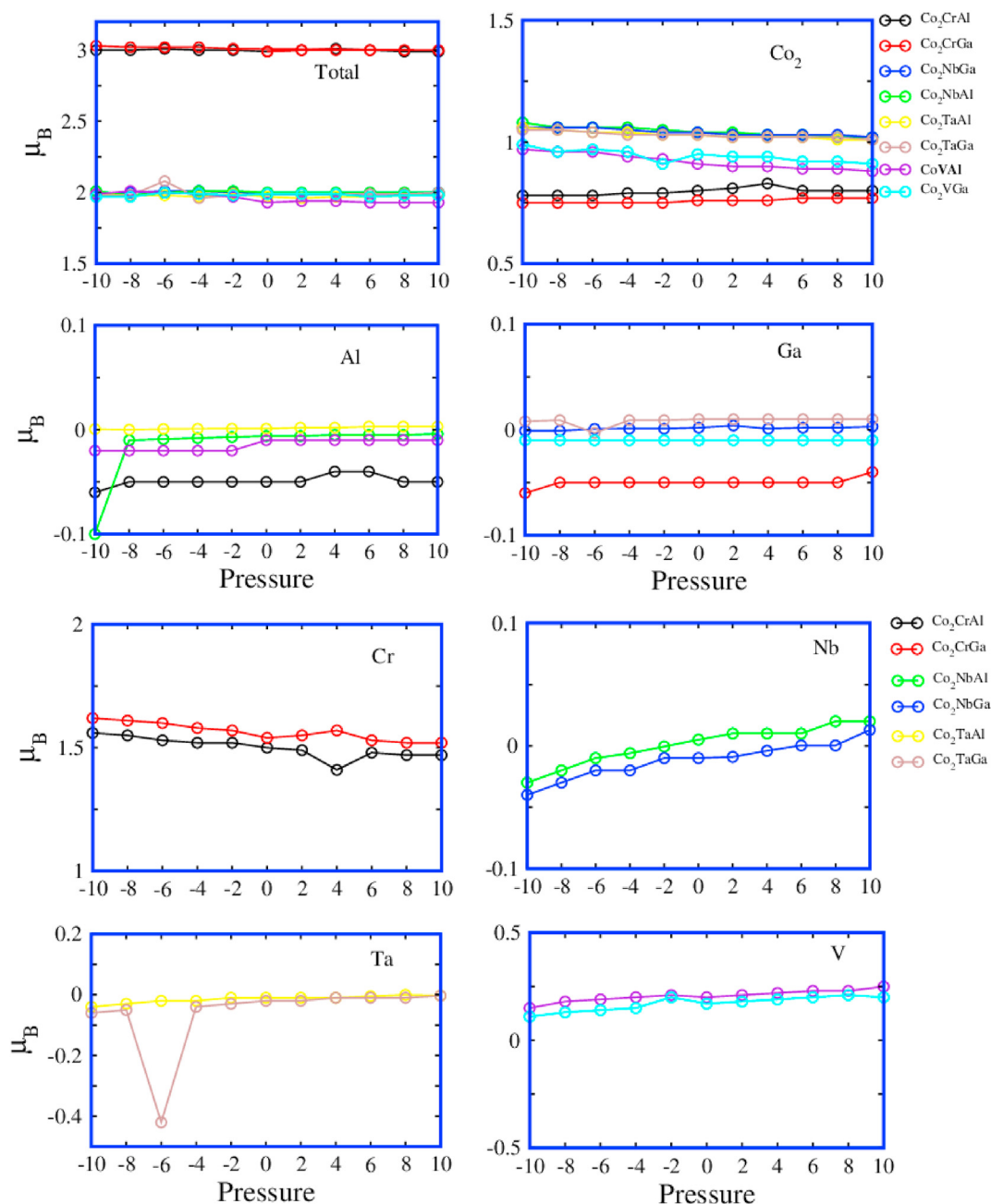
Fig. 10. Magnetic moments of the compounds under strained and unstrained conditions.

3.5.1. Optical conductivity under pressure

The optical conductivity of Co_2CrAl is given in Fig. S11. By gradually increasing pressure from 2 GPa to 10 GPa, the peak shifts towards slightly higher conductivities, maintaining the same trend of being more conductive in visible region and showing decrease in conductivity towards higher energies. The same trend is followed by the decrease in pressure going from -2GPa to -10GPa. The optical conductivity of Co_2CrGa is given in Fig. S12. In both of cases, the optical conductivity starts increasing towards the visible region from infrared region, having maximum conductivity for visible region and then shows a sharp decrease in conductivity towards higher energies. The optical conductivity of Co_2CrAl is given in Fig. S13. It shows a sharp increase towards visible region after which it decreases sharply towards higher energies showing comparatively less conductive behavior in ultraviolet region with slight changes in order of lines representing various pressures. The optical conductivity of Co_2NbGa is given in Fig. S14 Co_2NbGa follows the same trend as rest of the compounds, with conductivity increasing in infrared region towards visible region and after which it starts decreasing towards the higher energies. The optical conductivity of Co_2TaAl is given in Fig. S15. The maximum conductivity is found to be in visible region in both of the cases but when the pressure is decreased, the peaks shifts towards higher conductivity as compared to the case of increasing pressure. The optical conductivity of Co_2TaGa is given in Fig. S16. In case of the increasing pressures the conductivity increases towards visible region and then starts decreasing towards higher energies. In the case of pressure reduction, for -6GPa, there is a shift in the peak toward lower conductivity in visible range after there is a sharp decrease in conductivity at higher energies which almost vanishes moving towards ultraviolet region. The optical conductivity of Co_2VAl is given in Fig. S17. There is a sharp increase in conductivity from infrared to visible region after which it decreases sharply towards higher energies. The compound being slightly conductive in ultraviolet region in both of the cases. The optical conductivity of Co_2VGa is given in Fig. S18. In both of the cases, the conductivity is found to be decreasing with increasing pressures as compared to the case when no pressure is applied. While in case the decreasing pressures there is shift in the order of the pressure lines. -2 GPa having slightly higher peak than others.

3.6. Magnetic properties

All the information about atom resolved moments, total spin magnetic moment, experimental and calculated moments are summarized in Table 3. For each compound, the calculations were carried out using optimized lattice parameters. In most of cases the spin magnetic moment is exactly an integer as expected for half metals. The calculated magnetic moments are in good agreement with experimental and other theoretical results values [27,30]. The calculated total spin magnetic moment of the compounds is combination of moments at A sites (2 times), B sites, C sites and the magnetic moment of interstitials between the sites (see Fig. 10). Based on magnetic moments, all the compounds are ferromagnets.

4. Conclusions

Density functional calculations were successfully performed using FP-LAPW + lo method utilized in the WIEN2k code. The structural, electronic, magnetic and optical properties of Full-Heusler alloys Co_2XY (X = Cr, Nb, Ta, V; Z = Al, Ga) were calculated. Calculated lattice constants are in reasonable agreement with the available data. It is determined that lattice constant deceases with the increase in tensile stress and increases by increasing pressure in reverse direction. These compounds are half metals

with direct band gaps in semiconducting state which depicts their potential uses in spintronics. The nature of the band (direct) remains intact with strain. The bond length decreases while band gap increases in compressive strain. The compounds are found to be reflective in visible region, as characteristics of the metals. In most of the cases, the magnetic moments are exactly integers as expected for half metals.

Declaration of competing interest

The authors declare that they have no known competing financial interests or personal relationships that could have appeared to influence the work reported in this paper.

Appendix A. Supplementary data

Supplementary data to this article can be found online at https://doi.org/10.1016/j.jmgm.2021.107841.

References

[1] A. Aznar, A. Gràcia-Condal, A. Planes, P. Lloveras, M. Barrio, J.L. Tamarit, W. Xiong, D. Cong, C. Popescu, L. Mañosa, Giant barocaloric effect in all-d-metal Heusler shape memory alloys, Physical Review Materials 3 (4) (2019), 044406.

[2] A. Ayuela, J. Enkovaara, K. Ullakko, R.M. Nieminen, Structural properties of magnetic Heusler alloys, J. Phys. Condens. Matter 11 (8) (1999) 2017.

[3] F. Heusler, Über magnetische manganlegierungen, Verhandlungen Dtsch. Phys. Ges. 5 (1903) 219.

[4] M. Yin, J. Hasier, P. Nash, A review of phase equilibria in Heusler alloy systems containing Fe, Co or Ni, J. Mater. Sci. 51 (1) (2016) 50−70.

[5] A. Boochani, H. Khosravi, J. Khodadadi, S. Solaymani, M.M. Sarmazdeh, R.T. Mendi, S.M. Elahi, Calculation of half-metal, debye and curie temperatures of Co_2VAl compound: first principles study, Commun. Theor. Phys. 63 (5) (2015) 641.

[6] S. Ullah, H.U. Din, G. Murtaza, T. Ouahrani, R. Khenata, S.B. Omran, Structural, electronic and optical properties of $AgXY_2$ (X= Al, Ga, in and Y= S, Se, Te), J. Alloys Compd. 617 (2014) 575−583.

[7] F. Dahmane, Y. Mogulkoc, B. Doumi, A. Tadjer, R. Khenata, S.B. Omran, D.P. Rai, G. Murtaza, D. Varshney, Structural, electronic and magnetic properties of Fe2-based full Heusler alloys: a first principle study, J. Magn. Magn Mater. 407 (2016) 167−174.

[8] S.V. Karthik, A. Rajanikanth, Y.K. Takahashi, T. Ohkubo, K. Hono, Microstructure and spin polarization of quaternary $Co_2Cr_{1-x}V_xAl$, $Co_2V_{1-x}Fe_xAl$ and $Co_2Cr_{1-x}Fe_xAl$ Heusler alloys, Acta Mater. 55 (11) (2007) 3867−3874.

[9] T. Kanomata, Y. Chieda, K. Endo, H. Okada, M. Nagasako, K. Kobayashi, R. Kainuma, R.Y. Umetsu, H. Takahashi, Y. Furutani, H. Nishihara, Magnetic properties of the half-metallic Heusler alloys Co_2VAl and Co_2VGa under pressure, Phys. Rev. B 82 (14) (2010) 144415.

[10] K.R.A. Ziebeck, P.J. Webster, A neutron diffraction and magnetization study of Heusler alloys containing Co and Zr, Hf, V or Nb, J. Phys. Chem. Solid. 35 (1) (1974) 1−7.

[11] H. Han, G.Y. Gao, K.L. Yao, First-principles study on the half-metallicity of full-Heusler alloy Co_2VGa (111) surface, J. Appl. Phys. 111 (9) (2012), 093730.

[12] E.I. Gladyshevskii, Powder metallurgy and metal ceramics, Poroshkovaya Metallurgiya Kiev 1 (1962) 262.

[13] R.Y. Umetsu, K. Kobayashi, A. Fujita, K. Oikawa, R. Kainuma, K. Ishida, N. Endo, K. Fukamichi, A. Sakuma, Half-metallic properties of $Co_2(Cr_{1-x}Fe_x)$ Ga Heusler alloys, Phys. Rev. B 72 (21) (2005) 214412.

[14] E.I. Shreder, A.D. Svyazhin, K.A. Belozerova, Optical properties of heusler alloys Co_2FeSi, Co_2FeAl, Co_2CrAl, and Co_2CrGa, Phys. Met. Metallogr. 114 (11) (2013) 904−909.

[15] T. Kanomata, H. Nishihara, T. Osaki, M. Doi, T. Sakon, Y. Adachi, T. Kihara, K. Obara, T. Shishido, Magnetic properties of ferromagnetic Heusler alloy Co_2NbGa, J. Magn. Magn Mater. 503 (2020) 166604.

[16] M. Ayad, F. Belkharroubi, F.Z. Boufadi, M. Khorsi, M.K. Zoubir, M. Ameri, I. Ameri, Y. Al-Douri, K. Bidai, D. Bensaid, First-principles calculations to investigate magnetic and thermodynamic properties of new multifunctional full-Heusler alloy Co_2TaGa, Indian J. Phys. (2019) 1−11.

[17] M. Zhang, Z. Liu, H. Hu, G. Liu, Y. Cui, J. Chen, G. Wu, X. Zhang, G. Xiao, Is

Heusler compound Co_2CrAl a half-metallic ferromagnet: electronic band structure, and transport properties? J. Magn. Magn Mater. 277 (1−2) (2004) 130−135.

[18] J. Enkovaara, A. Ayuela, A.T. Zayak, P. Entel, L. Nordström, M. Dube, J. Jalkanen, J. Impola, R.M. Nieminen, Magnetically driven shape memory alloys, Mater. Sci. Eng. 378 (1−2) (2004) 52−60.

[19] H.P.J. Wijn, Alloys and compounds of 3d elements with main group elements, in: Magnetic Properties of Metals, Springer, Berlin, Heidelberg, 1991, pp. 95−158.

[20] A.H. Reshak, Transport properties of Co-based Heusler compounds Co_2VAl and Co_2VGa: spin-polarized DFT+ U, RSC Adv. 6 (59) (2016) 54001−54012.

[21] A.W. Carbonari, R.N. Saxena, W. Pendl Jr., J. Mestnik Filho, R.N. Attili, M. Olzon-Dionysio, S.D. De Souza, Magnetic hyperfine field in the Heusler alloys Co_2YZ (Y= V, Nb, Ta, Cr; Z= Al, Ga), J. Magn. Magn Mater. 163 (3) (1996) 313−321.

[22] Y. Li, H. Yuan, J. Xia, G. Zhang, M. Zhong, A. Kuang, G. Wang, X. Zheng, H. Chen, First-principles study on structural, electronic, elastic and thermodynamic properties of the full-Heusler alloys Co_2YZ (Y= Sc, Cr and Z= Al, Ga), Eur. Phys. J. Appl. Phys. 70 (3) (2015) 31001.

[23] S. Nepal, R. Dhakal, I. Galanakis, Ab initio study of the half-metallic full-Heusler compounds Co_2ZAl (Z= Sc, Ti, V, Cr, Mn, Fe); the role of electronic correlations, Materials Today Communications 25 (2020) 101498.

[24] D.P. Rai, R.K. Thapa, A half-metallic ferromagnetism study of Co_2YAl (Y= Zr, Nb, Hf) based on GGA, Journal of Spintronics and Magnetic Nanomaterials 1 (2) (2012) 97−103.

[25] P. Blaha, K. Schwarz, G.H. Madsen, D. Kvasnicka, J. Luitz, FP-L/APW+lo Program for Calculating Crystal Properties, 2001. Schwarz, K.; Techn. WIEN2k, Austria.

[26] R.A. De Groot, F.M. Mueller, P.G. Van Engen, K.H.J. Buschow, New class of materials: half-metallic ferromagnets, Phys. Rev. Lett. 50 (25) (1983) 2024.

[27] H.C. Kandpal, G.H. Fecher, C. Felser, Calculated electronic and magnetic properties of the half-metallic, transition metal based Heusler compounds, J. Phys. Appl. Phys. 40 (6) (2007) 1507.

[30] K.A. Fomina, V. Marchenkov, E.I. Shreder, H.W. Weber, Electrical and optical properties of X_2YZ (X= Co, Fe; Y= Cr, Mn, Ti; Z= Ga, Al, Si) Heusler alloys, in: Solid State Phenomena, vol. 168, Trans Tech Publications Ltd, 2011, pp. 545−548.